Research Article

Xiao Hu*, Li Xie*, Zhenlin Chen, Pengcheng Lei, Hao Chen, and Tao Tan

Study on the uniaxial compression constitutive relationship of modified yellow mud from minority dwelling in western Sichuan, China

https://doi.org/10.1515/rams-2022-0291
received September 03, 2022; accepted December 14, 2022

Abstract: More than 2 billion people around the world still use raw earth architecture, in countries like Nepal, India, and Iran. In China, the proportion of people living in earthen structures rose to 36%, some of them in western Sichuan. Minority dwellings in western Sichuan, China, use local stone and yellow mud as building materials and have been used for thousands of years. Because yellow mud is a brittle material with poor mechanical properties, and because the region is prone to earthquakes, the walls are highly susceptible to damage under seismic action. To improve the mechanical properties of yellow mud, the yellow mud of Taoping Qiang Village in western Sichuan was studied and modified. Uniaxial compressive tests were conducted on the modified specimens, and the existing ontogenetic equations of raw soil-based materials were analyzed and optimized. Finally, we developed the constitutive models for yellow clay and modified yellow clay in the western Sichuan area, which can be used for different kinds of modified materials through the variation of parameters. The results show that the compressive strength of yellow clay is improved by adding the modified materials. The optimized constitutive model can better fit the test curves, which can provide a basis for theoretical calculations and seismic mitigation of minority residential structures in western Sichuan or similar structural systems.

* **Corresponding author: Xiao Hu,** State Key Laboratory of Geohazard Prevention and Geoenvironment Protection, Chengdu University of Technology, Chengdu 610059, China, e-mail: huxiao@cdut.cn
* **Corresponding author: Li Xie,** State Key Laboratory of Geohazard Prevention and Geoenvironment Protection, Chengdu University of Technology, Chengdu 610059, China, e-mail: xieli918@126.com
Zhenlin Chen, Pengcheng Lei, Hao Chen, Tao Tan: State Key Laboratory of Geohazard Prevention and Geoenvironment Protection, Chengdu University of Technology, Chengdu 610059, China

Keywords: Tibetan and Qiang dwelling, yellow mud, modified material, compressive strength, constitutive equation, curve fitting

1 Introduction

Since the cities were built, raw soil has been used as a building material, mainly for raw soil buildings and raw soil stone masonry buildings. It is estimated that 30% of the world's population currently lives or works in soil structures, such as in the monastery of Khachod Thupten Samprin in Nepal [1], the monastery of Kichu Lhakhang in Bhutan [1], Vélez Castle in Mula [2], and the town of Bam in Iran [3], etc. In China, the proportion of the population living in soil structures rose to 36%, such as Hakka Tulou in Fujian [4], Tupac houses in Yunnan [5], Tibetan and Qiang villages in western Sichuan, and so on. This research mainly focuses on yellow mud, the building material of ethnic minority dwellings in western Sichuan, China.

The Tibetan and Qiang minorities in western Sichuan, China, mainly live in Aba Autonomous Prefecture. The residential buildings of the Qiang ethnic minority in Tibet are part of the traditional architectural culture of the Chinese nation, with unique architectural forms and styles (Figure 1). Tibetan and Qiang-style architecture is China's indigenous architectural culture, and with continuous improvement and development, it is still in use today [8]. Due to the unique climatic conditions, geographical location and religious beliefs, this area has formed a special architectural form. Such buildings can adapt to local conditions, conform to the living habits of local residents, and have strong religious and ethnic characteristics. Therefore, the protection and reinforcement of Tibetan and Qiang-style buildings is an important part of promoting Chinese minority culture [6,7].

Most of the local buildings are made of raw masonry, and the walls are made of yellow mud as the bonding material. Aba Autonomous Prefecture belongs to the

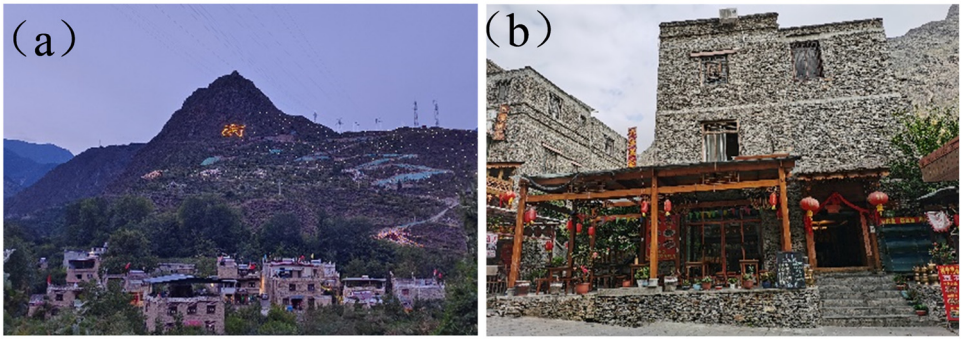

Figure 1: Tibetan and Qiang folk houses in western Sichuan: (a) Tibetan Village and (b) Qiang Village.

earthquake-prone area, and has experienced three earthquakes of magnitude 7.0 or above in the past 20 years. The results of the post-earthquake investigations showed that the earthquake damage to local houses was generally severe, with the main types of damage being wall cracks, loss of topsoil from the walls, and wall collapse (Figure 2). Many places in Aba Autonomous Prefecture have large altitude differences, complex topography, abnormal climate, and high rainfall. Due to the geographical location and climatic environment, the strength of yellow mud in western Sichuan is low, and the water resistance and scouring resistance are poor. Over time, the yellow mud is easy to fall off and makes the walls damaged [8–12]. Therefore, the study of the yellow mud in western Sichuan is an important part of protecting the dwellings of local ethnic minorities.

Yellow mud is a kind of raw soil material. Traditional raw soil materials have low flexural strength and poor ductility, and are typical brittle materials. The compressive strength of the material plays an important role in improving the mechanical properties of the raw soil masonry and the seismic performance of the raw soil wall. At present, many scholars at home and abroad have studied different modified materials to improve the physical and mechanical properties of raw soil materials, and certain research results have been achieved [13–15]. Zhao and Zheng [16], Li *et al.* [17], and Zhang *et al.* [18] found that fibers could improve soil strength with an optimum dose of 0.3%. Qu *et al.* [19] concluded that the larger the particle size of polystyrene, the more effective it is in improving soil strength. Shen *et al.* [20] found that the addition of either lime or cement significantly improved the strength and strength parameters at a certain fiber content, with cement showing better improvement than lime. Rivera *et al.* [21] found that it was technically feasible to produce blocks replacing conventional pavers using natural soil as the basic raw material and low-quality fly ash as the precursor, using an alkaline activation process.

At present, research on soil-building mainly focus on the modification of soil-material and the improvement of seismic performance of components [22–26]. Few people have studied the constitutive relation of raw soil materials. Zhao *et al.* [27] modified the raw soil with coarse

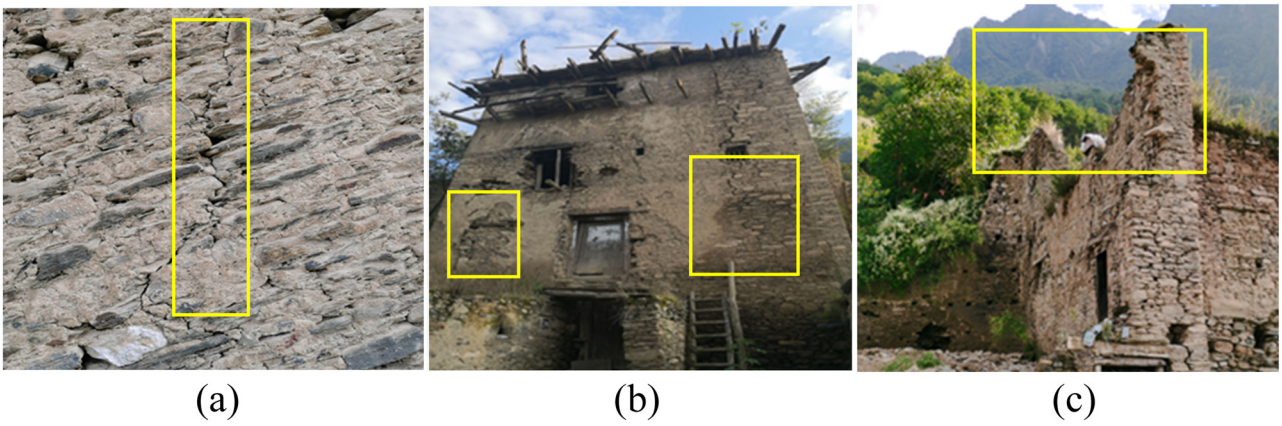

Figure 2: Disease status of Qiang Village wall: (a) wall cracks, (b) wall surface soil falling off, and (c) wall collapse.

sand and wheat straw and conducted uniaxial compression tests to establish the uniaxial constitutive equations for raw soil materials by fitting the relationships using rational equations and concrete materials. Ji [28] established a unified intrinsic constitutive model for raw soil-based materials in the form of segmental functions based on the stress–strain curves obtained from the tests. Zhang *et al.* [29] performed uniaxial compressive tests on raw soil specimens with different admixtures and ratios, and based on the test results, a dimensionless formula for the constitutive relationship was proposed using a unified formula, but applicable to raw soils of the loess plateau as well as cement soil. Guo [30] conducted uniaxial compressive tests on specimens mixed with different modified materials and modified the constitutive relationship for the raw soil material. Illampas *et al.* [31] established the constitutive equations for raw earth materials by uniaxial compression tests on adobe bricks, but only for adobe bricks mixed with straw. The properties of raw soil materials vary greatly in different regions. Because of the characteristics of yellow mud in western Sichuan, the existing constitutive equation is not applicable. Aba Autonomous Prefecture is an earthquake-prone area, so it is urgent to design and transform its components and structures. The constitutive relation of modified yellow mud is the basic work of seismic performance of structures. Therefore, it is an important content to establish the constitutive equation of yellow mud in western Sichuan.

The straw output in China's countryside area is huge, and its current processing method mostly does not conform to the environmental protection requirements [32]. To recycle it, straw is chosen as a kind of modifying material in this work. As a natural renewable resource, starch has been used in many fields because of its low price, adhesive film forming property and reducibility [33]. Therefore, starch is also selected as a modifying material in this work. Epoxy resin has good chemical properties and corrosion resistance, which is mostly used in the restoration of some ancient buildings, but rarely used in the improvement of raw soil materials [34]. Therefore, this work chooses epoxy resin as a kind of improving material. After investigation, it was found that the yellow mud had been completely replaced by cement in the stockade built in recent years, which destroyed the style of the local minority dwellings. In this work, cement is also selected as the material for this study to explore a suitable amount of cement to be added to yellow mud so as to improve the performance of yellow mud without destroying its original style. Based on this, four kinds of materials including straw, starch, cement, and epoxy resin were used to modify the yellow mud.

In summary, yellow mud in western Sichuan has disadvantages such as poor mechanical properties, poor water resistance, and weak scouring resistance, which lead to the easy destruction of minority houses in this region under earthquake effects. The compressive strength has become a basic value to measure the quality of material, so this time, straw, starch, cement, and epoxy resin were used to modify the yellow mud, and the effect of different materials on the compressive strength of yellow mud was studied by uniaxial compressive test to obtain the optimal admixture of each material. Due to the large dispersion of raw soil materials and regional differences, there are not many studies on the compressive constitutive relationship of raw soil materials at home and abroad. Part of the fit is based on the concrete constitutive relationship, and part of it is only applicable to raw soils in specific places and soils modified with specific materials and does not apply to the constitutive relationship of such raw soil masonry structures. Combining the stress–strain curves obtained from the tests and the previous studies, the compressive principal structure relationship of the raw soil material was further optimized and a constitutive model applicable to yellow clay in the western Sichuan area was derived. The obtained research results can provide a basis for theoretical calculations and seismic mitigation of the residential structures of minority groups in western Sichuan or similar structural systems.

2 Materials and methods

2.1 Materials

The raw materials for the test are taken from yellow mud on a hillside in Taoping Qiangzhai in Lixian County. Before making the test block, the yellow mud is dried under natural conditions for 1–2 days and then crushed so that it can pass through a 5 mm sieve. The yellow mud used is silty clay, mainly containing quartz, albite, kaolinite, calcite, and Illite, and other basic physical indicators are shown in Tables 1 and 2 and Figure 3.

Straw, starch, cement, and epoxy resins are selected as modifying materials (all purchased online). The length of the straw is between 3 and 4 cm, the surface is rough, and it has large friction. Starch is obtained from sweet potato, the color is white, with excellent adhesion to the film, and degradability. The cement is made of Portland cement, and the main chemical components are SiO_2, Al_2O_3, CaO, Fe_2O_3, MgO, SO_3, P_2O_5, Na_2O, etc. Epoxy resin adopted was of model E-51 and the curing agent is T-31,

Table 1: Particle size distribution

Particle distribution (%)	<0.075 mm	0.075–0.25 mm	0.25–0.5 mm	0.5–1 mm	1–2 mm	>2 mm
	72.56	2.64	2.85	4.67	6.30	10.98

Table 2: Basic physical property indexes of yellow mud

Natural moisture content (%)	Optimal moisture content (%)	Maximum dry density ($g \cdot cm^{-3}$)	Liquid limit (%)	Plastic limit (%)	Plasticity index
1.82	19.47	1.68	29.27	18.67	10.6

which is rationed according to 4:1, with stable chemical properties, strong adhesion, and low shrinkage.

2.2 Testing program

2.2.1 Preparation of samples

The test blocks were divided into 17 groups, 3 in each group, 51 in total, and the moisture content was 19.47%. Before starting production, the mold is coated with oil to facilitate mold release. When the yellow mud is mixed with the modifying material, it is manually stirred for 10–15 min. During the production process, a small vibrator is used to vibrate so that the modified material can be filled in the mold as much as possible and prevent hollowing inside the test block. After the trial blocks are made, they are released after 7 days of indoor maintenance, and then continue to be maintained for 28 days

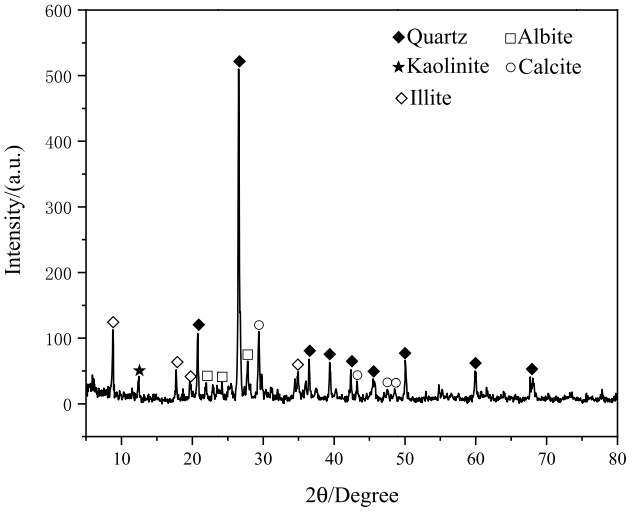

Figure 3: XRD pattern of yellow mud.

Figure 4: Image of samples produced for testing.

(Figure 4). The material ratio information on the test block is shown in Table 3, and the main equipment and instruments of the test are shown in Table 4.

2.2.2 Cube compression test

The stress-controlled loading rate was selected, which was 0.5 $MPa \cdot s^{-1}$. Before the test begins, the pressure surface size of each test block should be recorded and prepressed three times to ensure that the equipment works normally. After the test begins, the test block is placed in the middle of the stage and the indenter is aligned, and

Table 3: Modifying material ratio (quantity ratio)

Numbering	Material	Dosage
A	Yellow mud	100%
B	Straw	0.25, 0.5, 0.75, and 1%
C	Starch	1, 3, 5, and 7%
D	Cement	2, 5, 8, and 11%
E	Epoxy resin	3, 5, 7, and 10%

Table 4: Main test instruments and equipment

Equipment	Model
Classifier	5 mm
Electronic scale	YP3002N
Specimen mold box	70.7 mm × 70.7 mm × 70.7 mm
Concrete vibration table	ZD/LX—PTP
Pressure testing machine	WHY-1000

the indenter is adjusted to start loading after slight contact with the test block, and the pressurization is stopped when the test block is destroyed.

3 Results

3.1 Destruction form

According to the test phenomenon, it can be seen that the test block is placed on the loading table smoothly before fracturing. When the loading started, cracks only appeared in the weak areas around and on the surface of the test block and did not go through the whole test block (Figure 5b). At the late stage of the test, with the increase of load, cracks gradually widen and penetrate the whole test block. The skin around the crack fell off severely and a "funnel" crack appeared (Figure 5c). Eventually, the test block loses its load-bearing capacity and is destroyed.

Figure 6 shows the failure diagram of the yellow clay test block and the modified test block. When the pure yellow mud test block is destroyed, there are many cracks, and the cracks are deep, and the soil block falls off dangerously. After adding the straw, the cracks in the test block have increased, but the soil block did not fall off severely due to the binding effect of the straw on the soil. After adding starch, the cracks on the test block were shallower and the cracks through were less. After the addition of cement and epoxy resin, the cracks of the test block were significantly reduced, and were distributed in the edge of the test block.

3.2 Comparative analysis of peak stress and strain

Figure 7 shows the peak stress and strain of the test block under different modified materials and dosages. Straw, starch, and epoxy resins showed a peak value in their

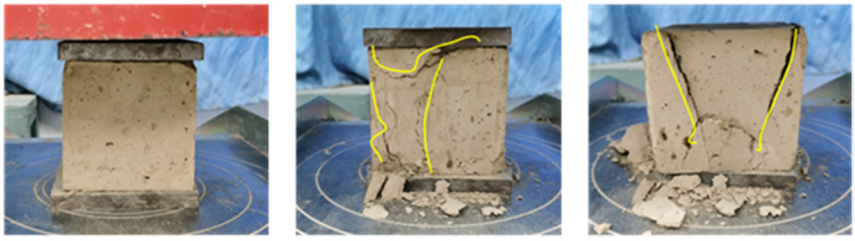

Figure 5: Cube compressive failure form; (a) prophase, (b) medium term, and (c) anaphase.

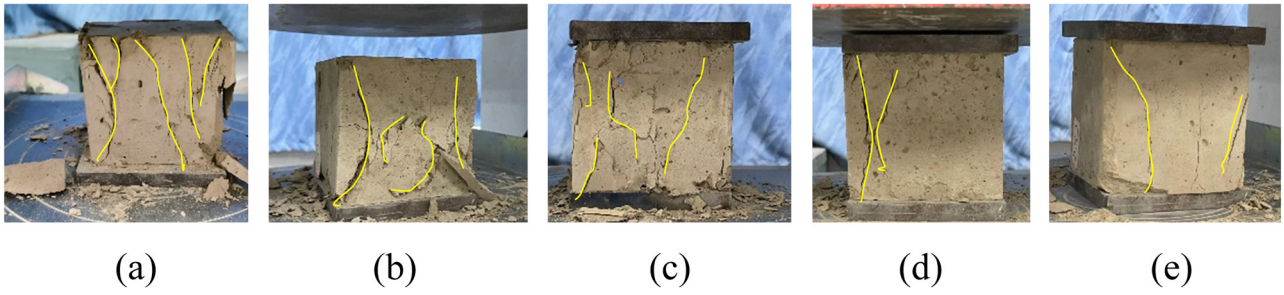

Figure 6: Destruction form of test block before modification: (a) yellow mud and after modifying using (b) straw, (c) starch, (d) cement, and (e) epoxy resin.

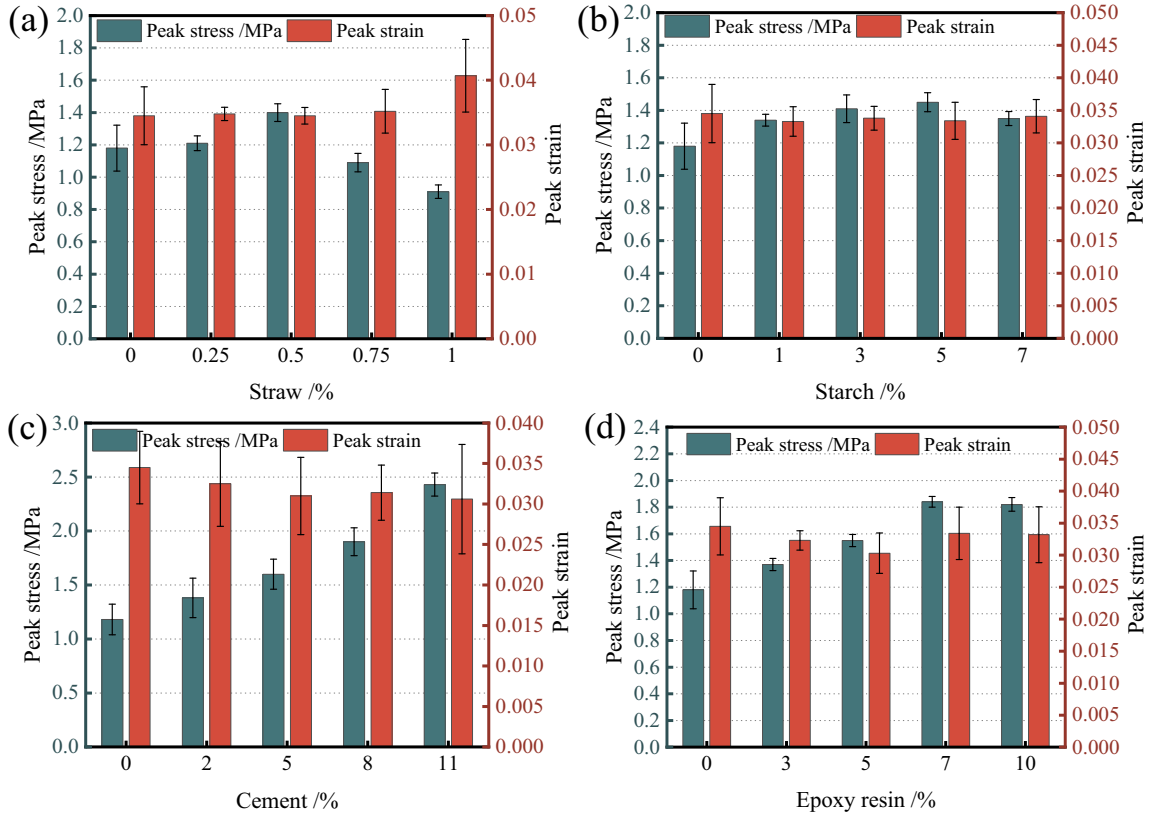

Figure 7: Peak stress and strain of test block. (a) straw; (b) starch; (c) cement; and (d) epoxy resin.

corresponding performance–content curves, while cement showed a unidirectional change.

As shown in the figure, the compressive strength of the test blocks showed a trend of increasing and then decreasing with the increase in straw and starch admixture. The compressive strength was 1.4 and 1.45 MPa, respectively, which increased by 18.64 and 22.88% compared with the pure yellow mud test block when the straw admixture was 0.5% and the starch admixture was 5%. With the increase in the content of epoxy resin, the compressive strength of the test block increased first and then decreased gradually. When the content of the epoxy resin is 7%, the strength reaches the peak, and the compressive strength of the test block is 1.84 MPa, which is 55.93% higher than that of the pure yellow mud test block. The compressive strength of the specimen increased with the increase in cement admixture. At 2, 5, 8, and 11% of cement admixture, the compressive strength of the test block was 1.38, 1.6, 1.9, and 2.43 MPa, respectively, which increased by 16.95–105.93% compared with the pure yellow mud test block. According to the Masonry Structure Design Code GB50003-2011, the strength standard of masonry mortar for rough stone masonry is 0.86 MPa multiplied by the safety factor of 1.77, the corresponding compressive strength value of 1.6 MPa at 5% cement admixture has met the local strength requirements. Combined with the current market price of cement, the cost required for different cement admixtures is increasing. Considering these two indicators, the improvement of the compressive strength of the cement on the yellow clay test block, the admixture amount is recommended to be controlled at 5%.

To compare the deformation ability of yellow mud mixed with different modified materials, the peak strain of the test block was analyzed (Figure 7). As shown in the figure, the peak strain of the test block is mostly between 0.0303 and 0.0352. The modified material improves the compressive strength of the test block, but has little influence on the peak strain, and can improve its dispersion, indicating that the modified raw soil has good homogeneity.

3.3 Test stress–strain full curve

According to the above analysis, the optimal doping amount of each modifying material was 0.5% for straw, 5% for starch, 5% for cement, and 7% for epoxy resin.

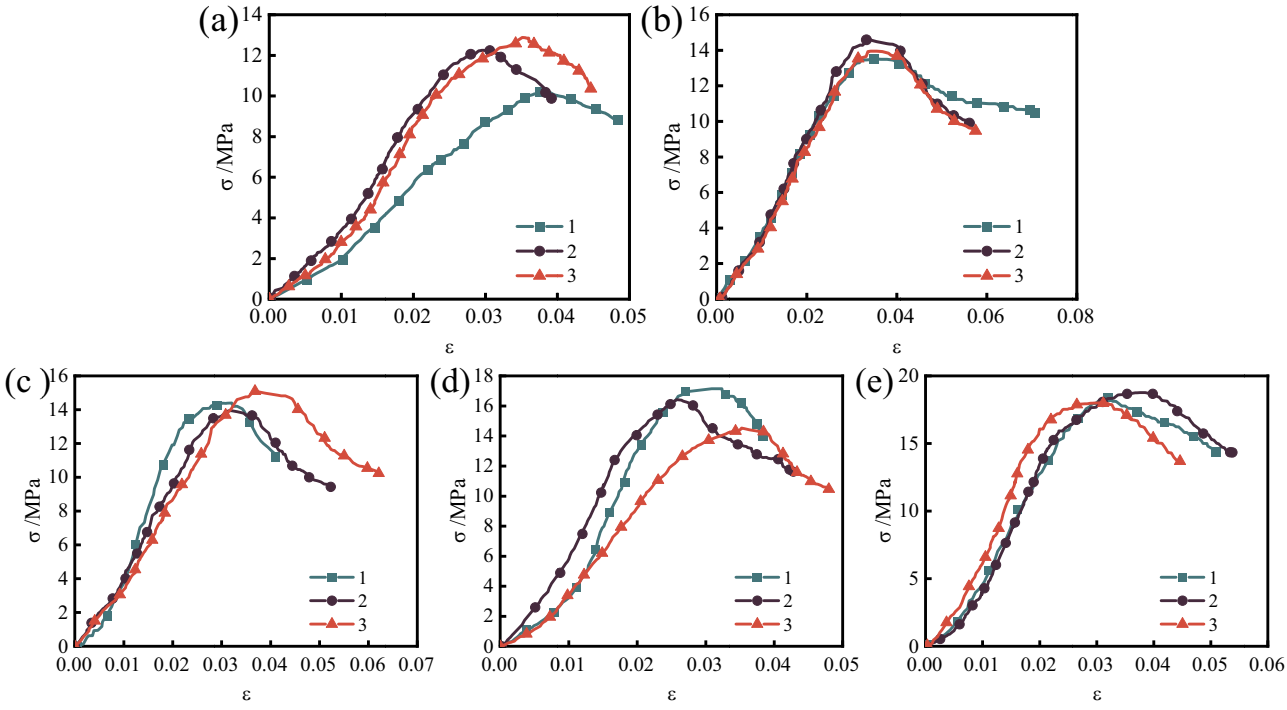

Figure 8: Stress–strain curve of test block: (a) yellow mud, (b) 0.5% straw, (c) 5% starch, (d) 5% cement, (e) 7% epoxy resin.

Figure 8 shows the stress–strain curves of the test blocks with the optimal doping amounts (the number in the legend is the trial block number).

As can be seen from the figure, the stress–strain curve of raw soil material is different from other construction materials in that there are two processes in the rising section. At the beginning of the rising section, there will be a down-concave section, and at the later stage, it will change to the up-convex section which is common in the curve of general construction materials, that is, the slope of the rising section curve will rise first and then fall. Analysis of the reason shows that the test block in the maintenance process will lose a lot of water, resulting in a large number of pores. During the loading process, the test block is gradually compacted, the pore space is reduced, and the pressure required to produce the same deformation is greater, which accelerates the growth of the slope at the beginning of the rising section of the curve. At the later stage, the pores in the test block are filled, the load rises faster, cracks appear in the test block, the deformation is accelerated, and the load reaches the limit and stops rising, the process is similar to the loading curve of concrete and sintered brick.

The typical stress–strain curve of uniaxial compression of raw soil-based materials was obtained by comprehensive analysis of the test results and the results of other scholars, as shown in Figure 9. The four points 1, 2, 3, and 4 on the curve have clear physical meanings. Point 1 is the end point of microcrack and void compaction. Point 2 is the macroscopic cracking point of the specimen. Point 3 is the peak strength point of the specimen. Point 4 is the end of the experiment. The specimen is divided into four main stages from compression to destruction: compression-density stage ($0 \le \varepsilon \le \varepsilon 1$), elastic growth stage ($\varepsilon 1 \le \varepsilon \le \varepsilon 2$), yielding stage ($\varepsilon 2 \le \varepsilon \le \varepsilon 3$), and destruction stage ($\varepsilon 3 \le \varepsilon \le \varepsilon 4$). In the compaction stage, the slope of the curve increases and shows a concave shape.

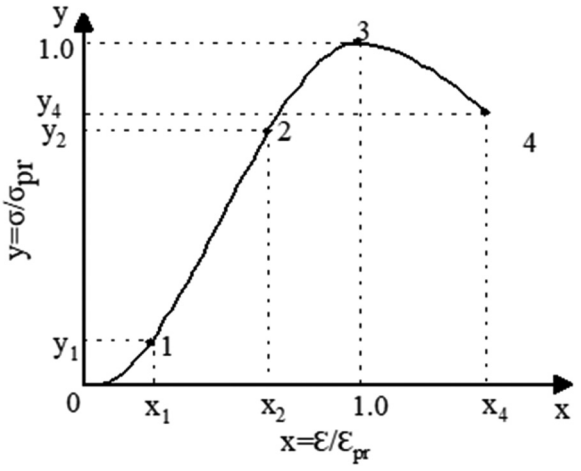

Figure 9: Typical stress–strain curve of raw soil material.

In the elastic growth stage, the slope of the curve is almost unchanged, showing a linear change. The slope of the curve decreases in the yield stage, and the slope is 0 at the peak point. When the strain reaches the peak point, the process is the destruction stage.

4 Compressive constitutive relationship of modified soil materials

4.1 Comparative analysis of existing constitutive equations

Most of the studies on the constitutive equations of raw soil materials use the results of uniaxial compressive tests to analogize the constitutive relationships of other construction materials to obtain suitable constitutive equations, which are generally divided into two parts. Table 5 shows the existing constitutive equations of raw soil materials. According to Table 5, the test curve of the pure yellow mud test block was selected for fitting, as shown in Figure 10.

Table 5: Constitutive equation of raw soil material

S. no.	Author	Equation	Note
1	Zhao C	$y = \frac{ax}{bx^2 + cx + 1}$	Full curve
2	Zhang YC	$y = \begin{cases} e^{-5.3(x-1)^2} \\ 1.5 - 0.5x \end{cases}$	$x \le 1$ $x \ge 1$
3	Rogiros Illampas	$y = \begin{cases} a_1x + b_1x^2 + c_1x^3 \\ a_2 + b_2x + c_2x^2 + d_2x^3 \end{cases}$	$x \le 1.07$ $1.07 \le x \le 4$

Zhao *et al.* [27] described the compressive constitutive relationship of the whole test block by the same equation, although the form is simple, the concave section at the beginning of the curve differs from the curve obtained from the test. Zhang *et al.* [29] expressed the constitutive relationship in the form of segmental functions, using the power exponential function and the primary function, respectively. Illampas *et al.* [31] also used segmented functions to express the instanton equation and both segments were cubic functions, which could better characterize the curve. However, the segmentation point is not at $x = 1$, but at $x = 1.07$, which is slightly different from the stress–strain curve of the raw soil material. From Figure 10(c), it can be seen that the present constitutive equation fits both the segments of the curve well, and the fit is only different at the peak point.

In summary, the constitutive equation of Illampas *et al.* [31] was selected for optimization and used for fitting the test curve.

4.2 Revision of constitutive equation

A reasonable constitutive relationship should satisfy the following conditions: (i) the constitutive relationship can fit the experimental results well; (ii) the formula is simple and applicable; and (iii) the parameters are few and the physical meaning is clear. After the above analysis of the constitutive equation proposed by Illampas *et al.* [31], Ji [28] referred to the geometric conditions of the concrete constitutive equation, described the geometric characteristics of the stress–strain full curve of soil-based materials with mathematical relations, and then deduced its constitutive equation. The curve obtained in this study also meets the requirements, so the method mentioned in the paper of Ji [28] is adopted to optimize it.

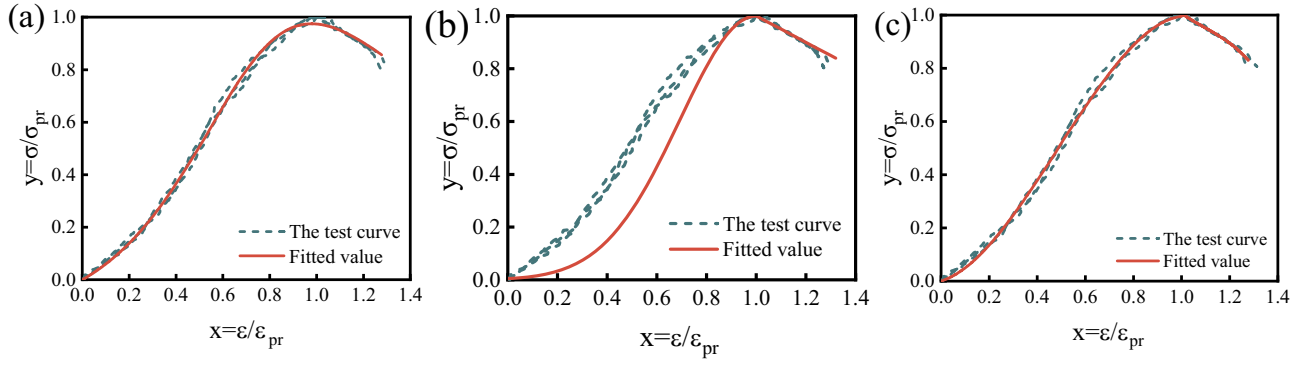

Figure 10: Comparison of constitutive models: (a) Zhao C, (b) Zhang YC, and (c) Rogiros Illampas.

The piecewise point is set at $x = 1$, and the geometric conditions for the establishment of the concrete intrinsic constitutive equation are borrowed: (i) $x = 0$, $y = 0$ and (ii) $y = 1$, $\frac{dy}{dx}|_{x=1} = 0$ at $x = 1$.

4.2.1 Curve of rising ($0 \le x \le 1$)

The rising segment of the constitutive equation proposed by Illampas *et al.* [31] is as follows:

$$y = a_1x + b_1x^2 + c_1x^3. \tag{1}$$

The first-order derivative is found for equation (1), and the result is shown in equation (2).

$$y' = a_1 + 2b_1x + 3c_1x^2. \tag{2}$$

Substituting geometric conditions $x = 0$, $y = 0$; $x = 1$, $y = 1$; $\frac{dy}{dx}|_{x=1} = 0$ in equations (1) and (2), the curve equation of the ascending section can be obtained as follows:

$$y = a_1x + (3 - 2a_1)x^2 + (a_1 - 2)x^3. \tag{3}$$

There is only one independent parameter a_1 left in the equation.

When $x = 0$, $\frac{dy}{dx} = a_1$ according to equation (2). The parameter a_1 can be expressed as:

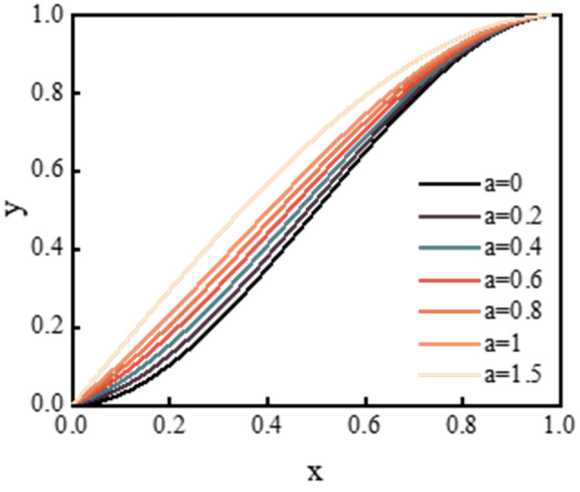

Figure 11: The influence of a_1 on the ascending segment curve.

$$a_1 = \frac{dy}{dx}|_{x=1} = \frac{d\sigma/\sigma_{pr}}{d\varepsilon/\varepsilon_{pr}}|_{x=1} = \frac{d\sigma/d\varepsilon|_{x=1}}{\sigma_{pr}/\varepsilon_{pr}} = \frac{E_0}{E_p}, \tag{4}$$

where $E_0 = d\sigma/d\varepsilon|_{x=1}$ is the initial tangent modulus of soil-based material (unit: N·mm^{-2}); $E_p = \sigma_{pr}/\varepsilon_{pr}$ is the secant modulus corresponding to the peak point of soil-based material (unit: N·mm^{-2}). The physical meaning of parameter a_1 is clear: it is the ratio of the initial tangent modulus to the peak secant modulus of the soil-based material.

The variation in the rising segment curve corresponding to different values of a_1 is shown in Figure 11. When $a_1 = 1$, the curve has no concave segment, which is not consistent with the stress–strain curve of the raw soil-based material. When the value of a_1 is smaller, the lower concave section is closer to the x-axis.

4.2.2 Descending segment curve ($x \ge 1$)

The descending segment of the instanton equation proposed by Illampas *et al.* [31] is as follows:

$$y = a_2 + b_2x + c_2x^2 + d_2x^3. \tag{5}$$

The first-order derivative is found for equation (5), and the result is shown in equation (6)

$$y' = b_2 + 2c_2x + 3d_2x^2. \tag{6}$$

Substituting geometric conditions $x = 1$, $y = 1$; $\frac{dy}{dx} | x = 1 = 0$ in equations (5) and (6), the curve equation of the ascending section can be obtained as follows:

$$y = (1 + c_2 + 2d_2) - (2c_2 + 3d_2)x + c_2x^2 + d_2x^3. \tag{7}$$

In summary, the optimized stress–strain relationship of soil-based materials can be expressed as follows:

$$y = \begin{cases} a_1x + (3 - 2a_1)x^2 + (a_1 - 2)x^3, & 0 \le x \le 1 \\ (1 + c_2 + 2d_2) - (2c_2 + 3d_2)x + c_2x^2 + d_2x^3, & x \ge 1. \end{cases} \tag{8}$$

Then, the uniaxial compression constitutive relation is as follows:

$$\frac{\sigma}{\sigma_{pr}} = \begin{cases} a_1\frac{\varepsilon}{\varepsilon_{pr}} + (3 - 2a_1)\left(\frac{\varepsilon}{\varepsilon_{pr}}\right)^2 + (a_1 - 2)\left(\frac{\varepsilon}{\varepsilon_{pr}}\right)^3, & 0 \le \varepsilon \le \varepsilon_{pr} \\ (1 + c_2 + 2d_2) - (2c_2 + 3d_2)\frac{\varepsilon}{\varepsilon_{pr}} + c_2\left(\frac{\varepsilon}{\varepsilon_{pr}}\right)^2 + d_2\left(\frac{\varepsilon}{\varepsilon_{pr}}\right)^3. & x \ge \varepsilon_{pr} \end{cases} \tag{9}$$

Table 6: Rising segment parameter values

Parameters	Yellow mud	0.5% straw	5% starch	5% cement	7% epoxy resin
a_1	0.167	0.276	0.393	0.214	0.627
R^2	0.995	0.993	0.987	0.993	0.982

Table 7: Descending segment parameter values

Parameters	Yellow mud	0.5% straw	5% starch	5% cement	7% epoxy resin
c_2	−37.841	−6.288	−28.403	−30.335	−11.473
d_2	10.940	1.543	8.083	8.416	3.025
R^2	0.959	0.965	0.985	0.961	0.980

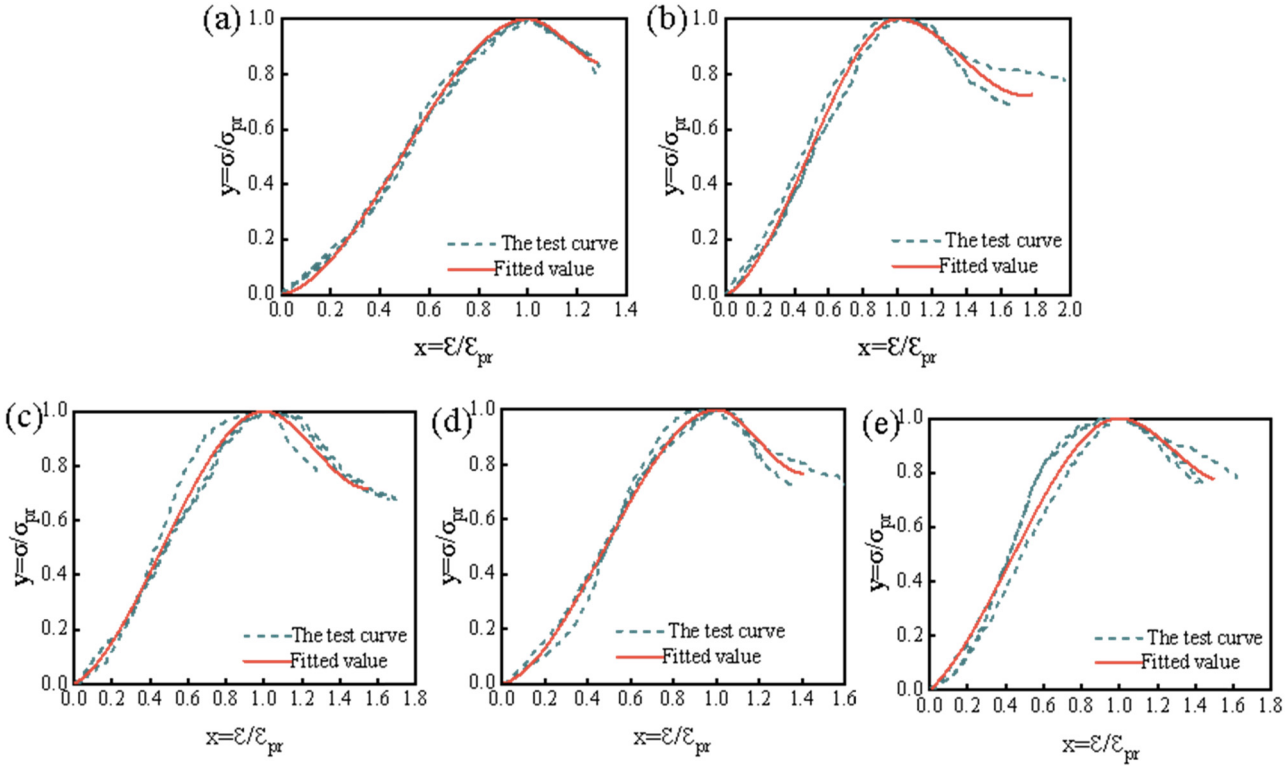

Figure 12: Comparison of experimental curve and fitted curve: (a) yellow mud, (b) 0.5% straw, (c) 5% starch, (d) 5% cement, and (e) 7% epoxy resin.

4.3 Comparison of theoretical formula with the experimental results

Based on the previous analysis of the experimental results, the optimal admixtures of each modified material were 0.5% straw, 5% starch, 5% cement, and 7% epoxy resin. The theoretical formula was fitted to the experimental results of these groups.

According to the optimized constitutive equation, to determine the parameter values of the constitutive equation corresponding to different modified materials, the stress–strain curves obtained in each group of tests were simplified into dimensionless stress–strain curves, and the software Origin was used for fitting. The results and effects of the fitting parameters are shown in Tables 6 and 7 and Figure 12. The corresponding parameter values of different modified materials are different, and the coefficients R^2 obtained by fitting are all greater than 0.95. Figure 12 shows that the ascending and descending segments of the curve obtained in the test have a good fitting effect, with basically the same shape and smooth and continuous curves, indicating that the optimized constitutive equation has a good fitting effect on the curve obtained in the test results. Therefore, this constitutive equation can better respond to the deformation characteristics of yellow mud in west Sichuan, China, and can provide support for the subsequent study.

5 Conclusion

Aiming at the shortcomings of low strength of yellow mud in Tibetan and Qiang dwellings, straw, starch,

cement, and epoxy resin are used as modifying materials to improve their strength. The compressive strength and constitutive relationship of soil-based materials are analyzed by combining experimental research and theoretical analysis. The main conclusions are as follows:

1) Straw, starch, cement, and epoxy resin all improved the compressive strength of Qiangzhai yellow mud, and the corresponding optimal dosages were 0.5, 5, 5, and 7%, respectively.
2) The modified material can improve the compressive strength of the test block, but has little effect on the peak strain. The discreteness can be improved, indicating that the homogeneity of the modified soil is better.
3) The optimized constitutive equation of raw soil-based materials can provide basic theoretical support for the subsequent theoretical calculation of the walls of ethnic minority dwellings in western Sichuan. The parameter a_1 of the constitutive equation has a clear physical and geometric meaning and reflects the relationship between the initial tangent modulus and the peak secant modulus of the raw soil-based material.

In this study, the properties of yellow mud modified by straw, starch, cement, and epoxy resin were studied, the existing constitutive equation of soil-based materials was modified, and the constitutive relationship applicable to yellow mud in western Sichuan was obtained, which provided a new idea for earthquake mitigation of Tibetan and Qiang dwellings in western Sichuan, China. The deficiency of this study lies in the small amount of experimental data and the limited applicability of the fitting formula. The constitutive relation is not applied to the seismic performance calculation of such structures. Follow-up studies will be strengthened.

Acknowledgments: This research is financially funded by State Key Laboratory of Geohazard Prevention and Geoenvironment Protection (No. SKLGP2020K010). Project is supported by Chinese Government Scholarship (CSC No. 201906560013). We thank our research classmates for their valuable work and providing experiment data and the anonymous reviewer for his critiques and comments.

Funding information: This study was supported by State Key Laboratory of Geohazard Prevention and Geoenvironment Protection (No. SKLGP2020K010). Project is supported by Chinese Government Scholar-ship (CSC No. 201906560013).

Author contributions: Xiao Hu and Li Xie: methodology, software, and manuscript writing. Li Xie, Pengcheng Lei, Hao Chen, and Tao Tan: experiment and simulation validation. Xiao Hu and Zhenlin Chen: supervision. Pengcheng Lei, Hao Chen, and Tao Tan: related research investigation. Li Xie: data processing and analysis. All authors have accepted responsibility for the entire content of this manuscript and approved its submission.

Conflict of interest: The authors state no conflict of interest.

References

[1] Jaquin, P. Influence of Arabic and Chinese rammed earth techniques in the Himalayan region. *Sustainability*, Vol. 4, No. 10, 2012, pp. 2650–2660.
[2] Arto, I., J. Garrido, and M. L. Gutierrez-Carrillo. Seismic vulnerability analysis of medieval rammed earth fortifications in southeastern Spain. *Bulletin of Earthquake Engineering*, Vol. 18, No. 13, 2020, pp. 5827–5858.
[3] Gomes, M. I., M. Lopes, and J. De. Brito. Seismic resistance of earth construction in Portugal. *Engineering Structures*, Vol. 33, No. 3, 2011, pp. 932–941.
[4] Luo, Y., B. T. Yin, X. Q. Peng, Y. Y. Xu, and L. Zhang. Wind-rain erosion of Fujian Tulou Hakka earth buildings. *Sustainable Cities and Society*, Vol. 50, 2019, id. 101666.
[5] Dong, J. Y. and H. Jin. The design strategy of green rural housing of Tibetan areas in Yunnan, China. *Renewable energy*, Vol. 49, 2013, pp. 63–67.
[6] Zhu, X. M., D. S. Huang, and Y. O. Zhang. Study on architectural landscape cultural representation and ecological wisdom of Zengtou Qiang Village in Lixian County, Sichuan Province. *Wireless Communications and Mobile Computing*, Vol. 2022, 2022, id. 8052958.
[7] He, G. L., Z. Wang, M. G. Wang, and Y. P. Hou. Genetic diversity and phylogenetic differentiation of southwestern Chinese Han: a comprehensive and comparative analysis on 21 non-CODIS STRs. *Scientific reports*, Vol. 7, No. 1, 2017, pp. 1–8.
[8] Traoré, L. B., C. Ouellet-Plamondon, A. Fabbri, F. McGregor, and F. Rojat. Experimental assessment of freezing-thawing resistance of rammed earth buildings. *Construction and Building Materials*, Vol. 274, 2021, id. 121917.
[9] Hou, S. W., H. Zhang, Y. Z. Zhang, X. Chen, and S. Y. Meng. Seismic vulnerability analysis of rural modified raw-soil structures. *Shock and Vibration*, Vol. 2021, 2021, id. 2839509.
[10] Zhou, T. G., Z. Y. Zhang, Z. F. Su, and P. Tian. Seismic performance test of rammed earth wall with different structural columns. *Advances in Structural Engineering*, Vol. 24, No. 1, 2021, pp. 107–118.
[11] An, J. W., G. Z.Nie, and B. Hu. Area-wide estimation of seismic building structural types in rural areas by using decision tree and local knowledge in combination. *International Journal of Disaster Risk Reduction*, Vol. 60, 2021, id. 102320.
[12] Li, X. L., Z. Q. Li, J. S. Yang, H. Y. Li, Y. H. Liu, B. Fu, et al. Seismic vulnerability comparison between rural Weinan and other rural areas in Western China. *International Journal of Disaster Risk Reduction*, Vol. 48, 2020, id. 101576.

[13] Colinart, T., T. Vinceslas, H. Lenormand, A. Hellouin DeMenibus, E. Hamard, and T. Lecompte. Hygrothermal properties of light-earth building materials. *Journal of Building Engineering*, Vol. 29, 2020, id. 101134.
[14] Walker, P., B. V. V. Reddy, and M. Mani. Preface for SI: Modern earth building materials and technologies. *Construction and Building Materials*, Vol. 262, 2020, id. 120663.
[15] Nguyen, T. D., T. T. Bui, A. Limam, T. H. Bui, and Q. B. Bui. Evaluation of seismic performance of rammed earth building and improvement solutions. *Journal of Building Engineering*, Vol. 43, 2021, id. 103113.
[16] Zhao, F. T. and Y. W. Zheng. Shear strength behavior of fiber-reinforced soil: experimental investigation and prediction model. *International Journal of Geomechanics*, Vol. 22, No. 9, 2022, id. 04022146.
[17] Li, L. H., T. B. Zang, H. L. Xiao, W. Q. Feng, and Y. L. Liu. Experimental study of polypropylene fibre-reinforced clay soil mixed with municipal solid waste incineration bottom ash. *European Journal of Environmental and Civil Engineering*, Vol. 2020, 2020, pp. 1–17.
[18] Zhang, J., W. Xu, P. W. Gao, L. H. Su, B. Kun, Y. Y. Li, et al. Integrity and crack resistance of hybrid polypropylene fiber reinforced cemented soil. *Journal of Engineered Fibers and Fabrics*, Vol. 17, 2022, id. 15589250211068428.
[19] Qu, J. L., H. Tao, W. Q. Qu, G. Q. Han, H. M. Liu, P. Abulimiti, et al. Modification of mechanical properties of Shanghai clayey soil with expanded polystyrene. *Science and Engineering of Composite Materials*, Vol. 29, No. 1, 2022, p. 37–49.
[20] Shen, Y. S., Y. Tang, J. Yin, M. P. Li, and T. Wen. An experimental investigation on strength characteristics of fiber-reinforced clayey soil treated with lime or cement. *Construction and Building Materials*, Vol. 294, 2021, id. 123537.
[21] Rivera, J. F., R. M. de Gutiérrez, S. Ramirez-Benavides, and A. Orobio. Compressed and stabilized soil blocks with fly ash-based alkali-activated cements. *Construction and Building Materials*, Vol. 264, 2020, id. 120285.
[22] Zhao, Y. Y., X. Z. Ling, W. G. Gong, P. Li, G. Y. Li, and L. N. Wang. Mechanical properties of fiber-reinforced soil under triaxial compression and parameter determination based on the Duncan-Chang model. *Applied Sciences*, Vol. 10, No. 24, 2020, id. 9043.
[23] Liu, C., Y. R. Lv, X. J. Yu, and X. Wu. Effects of freeze-thaw cycles on the unconfined compressive strength of straw fiber-reinforced soil. *Geotextiles and Geomembranes*, Vol. 48, No. 4, 2020, pp. 581–590.
[24] Xu, J. B., Y. Z. Luo, Y. Z. Wang, C. G. Yan, L. J. Zhang, L. H. Yin, et al. Triaxial axis shear mechanical properties of fiber-reinforced foamed lightweight soil. *Journal of Materials in Civil Engineering*, Vol. 33, No. 4, 2021, id. 04021047.
[25] Tang, H., H. H. Li, Z. Duan, C. Y. Liu, G. N. Wu, and J. Z. Luo. Direct shear creep characteristics and microstructure of fiber-reinforced soil. *Advances in Civil Engineering*, Vol. 2021, 2021, id. 8836293.
[26] Bai, X. Y., J. X. Ma, J. W. Liu, M. Y. Zhang, N. Yan, and Y. H. Wang. Field experimental investigation on filling the soda residue soil with liquid soda residue and liquid fly ash. *International Journal of Damage Mechanics*, Vol. 30, No. 4, 2021, pp. 502–517.
[27] Zhao, C., T. H. T. Akenjiang, J. Chen, and Y. J. Qin. Researches on modified raw-soil materials constitutive relation subject to uniaxial compression. *Journal of Xinjiang University* (*Natural Science Edition*), Vol. 27, No. 1, 2010, pp. 123–126 (in Chinese).
[28] Ji, Z. Q. *Study and application on constitutive relationship for earth material and mechanical compressed earth brick masonry* (*dissertation*). Chang'an University, Xian, 2018 (in Chinese).
[29] Zhang, Y. C., Y. H. Wang, N. N. Zhao, and T. Y. Wang. Experimental and stress-strain equation investigation on compressive strength of raw and modified soil in loess plateau. *Advances in Materials Science and Engineering*, Vol. 2016, 2016, id. 2681038.
[30] Guo, L. L. Experimental study on improving the performance of raw soil materials based on physical and chemical modification (dissertation). *Shi Hezi University*, Xin Jiang, 2021 (in Chinese).
[31] Illampas, R., I. Ioannou, and D. C. Charmpis. Adobe bricks under compression: Experimental investigation and derivation of stress–strain equation. *Construction and Building Materials*, Vol. 53, 2014, pp. 83–90.
[32] Lai, W. Y., S. J. Li, Y. A. Li, and X. H. Tian. Air pollution and cognitive functions: Evidence from straw burning in China. *American Journal of Agricultural Economics*, Vol. 104, No. 1, 2022, pp. 190–208.
[33] Costa, S., D. Summa, F. Zappaterra, R. Blo, and E. Tamburini. Aspergillus oryzae grown on rice hulls used as an additive for pretreatment of starch-containing wastewater from the pulp and paper industry. *Fermentation*, Vol. 7, No. 4, 2021, id. 317.
[34] Krzywinski, K., L. Sadowski, and M. Piechowka-Mielnik. Engineering of composite materials made of epoxy resins modified with recycled fine aggregate. *Science and Engineering of Composite Materials*, 28, 1, 2021, 276–284.